

Quantum efficiency of a microwave photon detector based on a current-biased Josephson junction

A. Poudel, R. McDermott, and M. G. Vavilov

Department of Physics, University of Wisconsin-Madison, Wisconsin 53706, USA

(Dated: January 17, 2012)

We analyze the quantum efficiency of a microwave photon detector based on a current-biased Josephson junction. We consider the Jaynes-Cummings Hamiltonian to describe coupling between the photon field and the junction. We then take into account coupling of the junction and the resonator to the environment. We solve the equation of motion of the density matrix of the resonator-junction system to compute the quantum efficiency of the detector as a function of detection time, bias current, and energy relaxation time. Our results indicate that junctions with modest coherence properties can provide efficient detection of single microwave photons, with quantum efficiency in excess of 80%.

PACS numbers: 85.25.Cp, 03.67.Lx, 03.65.Yz

Quantum optical photodetectors have contributed significantly to the development of quantum optics and atomic physics [1] and now play an essential role in optical quantum information applications such as quantum key distribution [2–4]. Recently, a novel paradigm for the study of radiation-matter interaction based on circuit quantum electrodynamics (cQED) has emerged as a test-bed for quantum optics in mesoscopic systems [5, 6]. In addition, cQED architectures are also an attractive candidate for scalable quantum computing and transmission of quantum information [7, 8]. Following the original proposal, a variety of cQED architectures demonstrating strong coupling between single photons and superconducting integrated circuits have been realized experimentally [9, 10]. This work has paved the way for the development of a superconducting microwave photon detector [11, 12] with possible applications to quantum information processing and communication [13].

The microwave photon detector is based on the current-biased Josephson junction (JJ): the JJ is biased so that absorption of a single microwave photon induces a transition to the voltage state, producing a large and easily detected classical signal [12]. While these detectors are straightforward to operate and show potential for scalability, performance is degraded by spurious dark counts due to quantum tunneling events in the absence of an absorbed photon; moreover, energy relaxation within the detector results in photon loss and leads to a reduction in measurement efficiency.

In this work, we theoretically determine the quantum efficiency of a microwave photon detector based on a current-biased JJ. Previous analysis [12, 14] of this system was focused on a continuous flux of photons incident on the detector. Here we study the probability of photon detection by a JJ coupled to a microwave mode that is loaded with a fixed number of photons. We solve the equation of motion for the density matrix of a resonator coupled to a JJ to obtain detector efficiency for different values of operation time, current bias, and relaxation

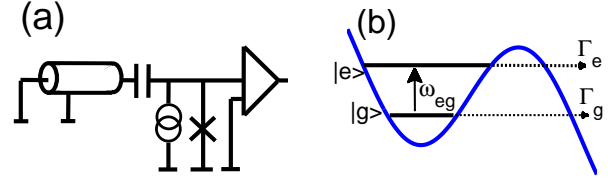


FIG. 1: (a) Schematic circuit diagram of JJ-based microwave photon detector coupled to a resonator. (b) Potential energy landscape of the detector when bias current is close to the critical current of the JJ. The junction is initialized in the $|g\rangle$ state and upon absorbing an incident photon transitions to the $|e\rangle$ state, which rapidly tunnels to the continuum.

time of the junction. Our results indicate a JJ with decay time around 10 ns can detect a single photon in the microwave mode with efficiency greater than 80% for readily achievable circuit parameters. We also find that the detector efficiency increases significantly with increase in energy relaxation time T_1 of the junction, suggesting that a highly efficient single microwave photon detector is attainable for a moderate improvement in junction quality.

The circuit diagram of the JJ and resonator system is shown in Fig. 1(a). The JJ is biased with a current I close to its critical value I_0 . The junction Hamiltonian can be written in terms of the charge operator \hat{Q} and the operator $\hat{\delta}$ of the phase difference across the JJ [15]:

$$\hat{H}_{JJ} = \frac{\hat{Q}^2}{2C} + U(\hat{\delta}), \quad U(\hat{\delta}) = -\frac{I_0 \Phi_0}{2\pi} \left(\cos \hat{\delta} - \frac{I}{I_0} \hat{\delta} \right). \quad (1)$$

Here C is the junction capacitance, $\Phi_0 = 2\pi\hbar/2e$ is the magnetic flux quantum, and \hbar and e are Planck's constant and the electron charge, respectively. For $I \lesssim I_0$, the potential energy landscape $U(\delta)$ takes on a “tilted washboard” shape, with a few discrete energy levels in shallow minima separated from the continuum by a barrier, see Fig. 1(b). We truncate the junction Hamiltonian to the ground $|g\rangle$ and first excited states $|e\rangle$ and obtain

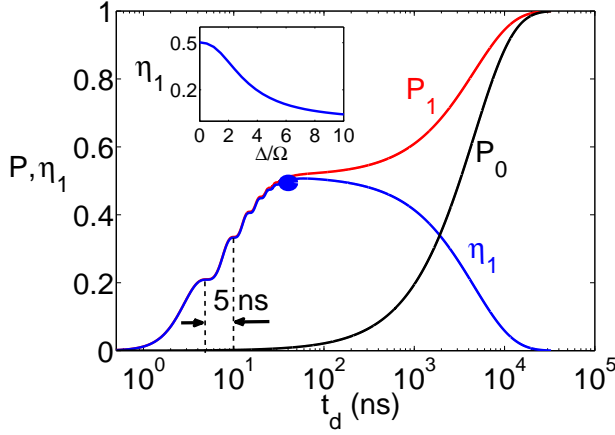


FIG. 2: (Color online) Switching probability P_1 (P_0) vs. photon detection time for initial states $|1, g\rangle$ ($|0, g\rangle$). Parameters used in this plot are: junction $T_1 = 10$ ns, barrier height $\Delta U/\hbar\omega_p = 2$, vacuum Rabi frequency $\Omega/2\pi = 100$ MHz, and cavity decay time $1/\kappa = 1$ μ s. Here the detuning between the resonator and the junction $\Delta = 0$. The solid blue curve is the quantum efficiency $\eta_1 \equiv P_1 - P_0$ (see the text). The maximum quantum efficiency of the detector is 50% for the optimal detection time of 40 ns (the optimal point is marked by a filled blue circle in the plot). In the inset, we plot the quantum efficiency vs. detuning Δ/Ω for the optimal detection time $t_d = 40$ ns obtained at $\Delta = 0$. The bandwidth of the detector is around 3.4Ω .

the following Hamiltonian for the JJ:

$$\hat{H}_{JJ} = \hbar\omega_{eg}\hat{\Pi}_e, \quad (2)$$

where $\hat{\Pi}_e = |e\rangle\langle e|$ is the projection operator to the excited state and $\omega_{eg} = (\varepsilon_e - \varepsilon_g)/\hbar$.

The Hamiltonian of a single mode microwave resonator with resonant frequency ω_r is given by

$$\hat{H}_r = \hbar\omega_r (\hat{a}^\dagger\hat{a} + 1/2), \quad (3)$$

where \hat{a}^\dagger (\hat{a}) is the creation (annihilation) operator of the resonator. The coupling of the resonator with the junction

is modeled by the Jaynes-Cummings (JC) Hamiltonian [16]:

$$\hat{H}_{JC} = \hbar\omega_r \left(\hat{a}^\dagger\hat{a} + \frac{1}{2} \right) + \hbar\omega_{eg}\hat{\Pi}_e + \hbar\Omega(\hat{a}^\dagger\hat{\sigma}_- + \hat{a}\hat{\sigma}_+), \quad (4)$$

where Ω is the vacuum Rabi frequency and $\hat{\sigma}_+$ ($\hat{\sigma}_-$) is the junction creation (annihilation) operator.

Our goal is to describe the time evolution of the density matrix $\hat{\rho}(t)$ for the resonator and the junction. We represent the density matrix in the basis $\{|n, j\rangle\}$, where n measures the number of photons in the resonator, and $j \in \{g, e\}$ represents the ground or excited state of the junction. We describe coupling of the system to its environment in terms of phenomenological decay rates. The coupling of the resonator with the environment produces a resonator decay rate $\kappa = \omega_r/Q$, where Q is the quality factor of the resonator. Similarly, finite dissipation in the JJ induces decay of the excited state with rate $\gamma \simeq 1/RC$ (decay time $T_1 = 1/\gamma$), where R represents the effective damping in the junction. The time evolution of the density matrix $\hat{\rho}(t)$ is governed by the following equation:

$$\frac{d\hat{\rho}(t)}{dt} = \frac{1}{i\hbar} [\hat{H}_{JC}, \hat{\rho}(t)] + \hat{\mathcal{L}}_\gamma[\hat{\rho}(t)] + \hat{\mathcal{L}}_\kappa[\hat{\rho}(t)] + \hat{\mathcal{L}}_T[\hat{\rho}(t)], \quad (5)$$

where $\hat{\mathcal{L}}_\gamma[\hat{\rho}(t)]$ and $\hat{\mathcal{L}}_\kappa[\hat{\rho}(t)]$ are superoperators that capture damping in the junction and the resonator at low temperatures $T \ll \hbar\omega_{eg}$, $\hbar\omega_r$ [17]:

$$\hat{\mathcal{L}}_\kappa[\hat{\rho}(t)] = \kappa \left(\hat{a}\hat{\rho}\hat{a}^\dagger - \frac{1}{2}\{\hat{a}^\dagger\hat{a}, \hat{\rho}\} \right), \quad (6a)$$

$$\hat{\mathcal{L}}_\gamma[\hat{\rho}(t)] = \gamma \left(\hat{\sigma}_-\hat{\rho}\hat{\sigma}_+ - \frac{1}{2}\{\hat{\sigma}_+\hat{\sigma}_-, \hat{\rho}\} \right). \quad (6b)$$

To account for switching of the ground and the first excited states of the junction to the voltage state, we introduce the tunneling superoperator $\hat{\mathcal{L}}_T[\hat{\rho}(t)]$ [18, 19]:

$$\hat{\mathcal{L}}_T[\hat{\rho}(t)] = - \begin{pmatrix} \Gamma_e\rho_{ee}^{nn} + \frac{\sqrt{\Gamma_e\Gamma_g}}{2}(\rho_{eg}^{nm} + \rho_{ge}^{nm}) & \frac{\Gamma_e + \Gamma_g}{2}\rho_{eg}^{nm} + \frac{\sqrt{\Gamma_e\Gamma_g}}{2}(\rho_{ee}^{nm} + \rho_{gg}^{nm}) \\ \frac{\Gamma_e + \Gamma_g}{2}\rho_{ge}^{nm} + \frac{\sqrt{\Gamma_e\Gamma_g}}{2}(\rho_{ee}^{nm} + \rho_{gg}^{nm}) & \Gamma_g\rho_{gg}^{nn} + \frac{\sqrt{\Gamma_e\Gamma_g}}{2}(\rho_{eg}^{nm} + \rho_{ge}^{nm}) \end{pmatrix}, \quad (7)$$

where $\Gamma_{e,g}$ are the tunneling rates from the ground, $|g\rangle$, and first excited, $|e\rangle$ states of the junction.

The system is originally prepared in a pure state $\hat{\rho}_n(0) = |n, g\rangle\langle n, g|$ with n photons in the cavity and the junction in the ground state $|g\rangle$. We numerically

solve the above equation for time evolution of the density matrix to compute occupation probabilities of the resonator and junction states. The probability that the JJ has switched to the voltage state at time t is given by

$$P_n(t) = 1 - \text{Tr}[\hat{\rho}_n(t)]. \quad (8)$$

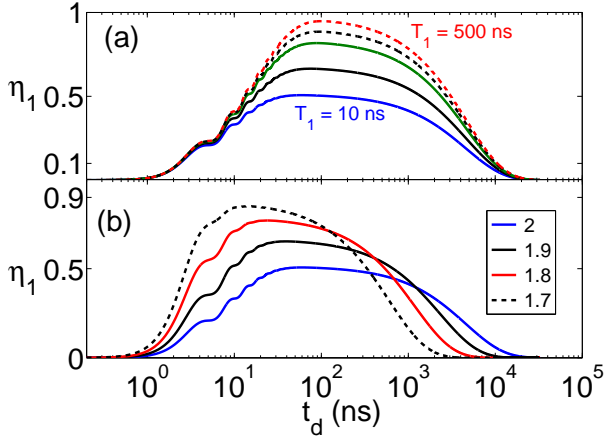


FIG. 3: (Color online) (a) Quantum efficiency η_1 vs. photon detection time for $\Delta U/\hbar\omega_p = 2$ and for various decay times of the junction: $T_1 = 10$ ns (solid blue), $T_1 = 20$ ns (solid black), $T_1 = 50$ ns (solid green), $T_1 = 100$ ns (dotted black), and $T_1 = 500$ ns (dotted red). For decay time of 500 ns, the maximum quantum efficiency is 94%. (b) Quantum efficiency η_1 vs. photon detection time for junction $T_1 = 10$ ns for various bias points of the junction: $\Delta U/\hbar\omega_p = 2$ (solid blue), 1.9 (solid black), 1.8 (solid red) and 1.7 (dashed black). The maximum quantum efficiency is 84% for $\Delta U/\hbar\omega_p = 1.7$. The remaining parameters are as in Fig. 2.

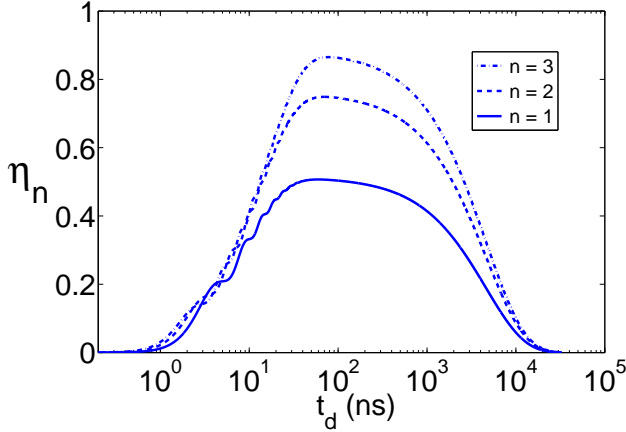


FIG. 4: (Color online) Efficiency η_n to detect a photon vs. detection time for $n = 1$ (solid blue), 2 (dashed blue), and 3 (dash-dotted blue) photons in the resonator. The rest of the parameters are as in Fig. 2. For three photons in the resonator, the efficiency to detect a photon is 85%.

We consider the following set of parameters for the JJ-resonator system, typical of those realized in experiments [12]: characteristic frequency of the junction $\omega_{eg}/2\pi = 4.8$ GHz, junction decay rate $\gamma = 10^8$ s $^{-1}$, resonator decay rate $\kappa = 10^6$ s $^{-1}$, and vacuum Rabi frequency $\Omega/2\pi = 100$ MHz. The tunneling rate of the first excited state of the junction is approximated by: $\Gamma_e \approx 500\Gamma_g = 7.3 \times 10^7$ s $^{-1}$ [21].

In Fig. 2, we plot switching probabilities $P_1(t)$, $P_0(t)$ of

the junction for initial states $|1, g\rangle$ (solid red) and $|0, g\rangle$ (solid black), respectively. For this part of the simulation, we consider the parameter $\Delta U/\hbar\omega_p = 2$, where ω_p is the plasma frequency of the JJ, and the detuning between the resonator and the junction is set to zero, i.e., $\Delta \equiv \omega_r - \omega_{eg} = 0$. The switching probability P_1 in Fig. 2 features steps whose periodic occurrence is a manifestation of Rabi oscillations of the junction with period $\pi/\Omega = 5$ ns. This result is consistent with the picture that switching of the junction halts momentarily when the junction returns to the ground state in course of the Rabi oscillations.

Next, we discuss the presence of the wide plateau of P_1 in Fig. 2. The occurrence of this plateau can be understood from the fact that switching of the junction is briefly frozen when the junction relaxes to the ground state due to dissipation. The JJ then switches to the voltage state after time $\sim 1/\Gamma_g$, the characteristic time scale for switching of the junction in the case of zero photons. The height of this plateau can be estimated as $\Gamma_e/(\Gamma_e + \gamma) \approx 0.5$, which agrees with the numerical result in Fig. 2.

In order to determine the quantum efficiency of the detector, we must properly treat dark counts due to quantum tunneling from the $|0, g\rangle$ state in the absence of photon absorption. The quantum efficiency η_1 of the detector is defined as the difference between the switching probabilities for an initial state with one photon $P_1(t)$, and for an initial state with no photons $P_0(t)$: $\eta_1 \equiv P_1(t) - P_0(t)$. The quantum efficiency is shown in Fig. 2 by the solid blue curve. For our choice of parameters $\Gamma_e \simeq \gamma$, the detector has maximum efficiency of about 50% for the optimal detection time t_d around 40 ns.

Next, we examine the bandwidth of the Josephson microwave photon detector. Here, we vary the frequency ω_r of the resonator and compute the quantum efficiency of the detector for the optimal detection time t_d obtained at zero detuning $\Delta = 0$. The detector bandwidth is then given by the detuning at which the quantum efficiency of the detector reduces to half the efficiency obtained at zero detuning. For a dissipation-free junction, the detector bandwidth is approximately given by the vacuum Rabi frequency. However, in the presence of dissipation and tunneling, the first excited state of the junction is broadened by $\sim \gamma + \Gamma_e$. This broadening of the energy level roughly accounts for the increased bandwidth of the detector. We find that the bandwidth is a factor of 3.4 larger than the vacuum Rabi frequency for the parameters of the detector chosen for Fig. 2, as shown in the inset of Fig. 2, see inset.

Next, we analyze the effect of dissipation and bias point on the efficiency of the detector. In Fig. 3(a), we plot the quantum efficiency of the detector for different values of the junction relaxation time T_1 from 10 ns to 500 ns, keeping all other parameters the same as in Fig. 2. We find that the quantum efficiency increases with increasing

junction relaxation time T_1 and reaches 94% for $T_1 = 500$ ns.

The change in bias current I of the junction modifies the ratio of barrier height ΔU to the junction plasma frequency ω_p . Taking different values of this ratio, we compute the efficiency of the detector at fixed relaxation time $T_1 = 10$ ns; the results are shown in Fig. 3 (b). Upon decreasing the ratio $\Delta U/\hbar\omega_p$, the potential well becomes shallower, leading to enhanced tunneling of the first excited state. This in turn increases the efficiency of the detector. Our simulation results indicate that a significant improvement in the detector efficiency is achieved when the tunneling rate exceeds the dissipation rate of the junction. We find that for bias point $\Delta U/\hbar\omega_p = 1.7$, the efficiency of the detector is about 84% for detection time around 9 ns.

Finally, we analyze the efficiency of the detector when the resonator is loaded with $n > 1$ photons. Generalizing the previous case of a single photon, the efficiency to detect a single microwave photon in resonator loaded with n photons is given by $\eta_n = P_n(t) - P_0(t)$. In Fig. 4, we plot the efficiency at fixed bias point $\Delta U/\hbar\omega_p = 2$ and $T_1 = 10$ ns for different numbers of photons in the resonator: $n = 1$ (solid blue), 2 (dashed blue), and 3 (dash-dotted blue). We find that detection efficiency increases upon increasing the number of photons in the resonator and reaches 85% for three photons in the resonator. This result is consistent with previous studies [12, 14] that reported higher efficiency of the detector, for the same parameters as above, when a continuous flux of photons was incident on the detector. For the case of a single photon in the resonator, the detector returns to the ground state after the photon is absorbed by the environment, and no further excitation of the junction is possible. However, when multiple photons are present in the resonator, other photons are available to induce excitation if the junction relaxes, thereby increasing the probability of photon detection.

In conclusion, we have presented a model to determine the quantum efficiency of a microwave photon detector based on a current-biased JJ. We have demonstrated that the efficiency to detect a single photon loaded in the resonator has maximal value $\Gamma_e/(\Gamma_e + \gamma)$. We have also determined that the bandwidth of the detector is characterized by the sum of the vacuum Rabi frequency and the broadening of the first excited state of the JJ due to tunneling and relaxation processes. Our simulations indicate that for currently used JJ photon detectors, the quantum efficiency is about 50% for the bias point $\Delta U/\hbar\omega_p = 2$ and about 85% for $\Delta U/\hbar\omega_p = 1.7$. We have finally investigated the probability to detect a photon in the case of a multiphoton initial resonator state and have found that the detection efficiency quickly approaches 100% as the initial number of photons increases, consistent with previous studies [12, 14] of a continuous flux of photons incident on the detector.

We gratefully acknowledge discussions with Guilhem Ribeill. This work was supported by ARO and DOD W911NF-11-1-0030 and NSF Grant No. DMR-1105178.

-
- [1] D. Walls and G. Milburn, *Quantum Optics* (Springer-Verlag, Berlin, 1994).
 - [2] E. Knill, R. Laflamme, and G. J. Milburn, *Nature* **409**, 46 (2001).
 - [3] P. Kok, W. J. Munro, K. Nemoto, T. C. Ralph, J. P. Dowling, and G. J. Milburn, *Rev. Mod. Phys.* **79**, 135 (2007).
 - [4] R. H. Hadfield, *Nature Photonics* **3**, 696 (2009).
 - [5] A. Blais, R.-S. Huang, A. Wallraff, S. M. Girvin, and R. J. Schoelkopf, *Phys. Rev. A* **69** (2004).
 - [6] A. Wallraff, D. I. Schuster, A. Blais, L. Frunzio, R. S. Huang, J. Majer, S. Kumar, S. M. Girvin, and R. J. Schoelkopf, *Nature* **431**, 162 (2004).
 - [7] J. Majer, J. M. Chow, J. M. Gambetta, J. Koch, B. R. Johnson, J. A. Schreier, L. Frunzio, D. I. Schuster, A. A. Houck, A. Wallraff, et al., *Nature* **449**, 443 (2007).
 - [8] J. Q. You and F. Nori, *Phys. Rev. B* **68** (2003).
 - [9] A. A. Houck, D. I. Schuster, J. M. Gambetta, J. A. Schreier, B. R. Johnson, J. M. Chow, L. Frunzio, J. Majer, M. H. Devoret, S. M. Girvin, et al., *Nature* **449**, 328 (2007).
 - [10] I. Chiorescu, P. Bertet, K. Semba, Y. Nakamura, C. J. P. M. Harmans, and J. E. Mooij, *Nature* **431**, 159 (2004).
 - [11] G. Romero, J. J. Garcia-Ripoll, and E. Solano, *Phys. Rev. Lett.* **102** (2009).
 - [12] Y.-F. Chen, D. Hover, S. Sendelbach, L. Maurer, S. T. Merkel, E. J. Pritchett, F. K. Wilhelm, and R. McDermott, *Phys. Rev. Lett.* **107** (2011).
 - [13] N. Gisin, G. Ribordy, W. Tittel, and H. Zbinden, *Rev. Mod. Phys.* **74**, 145 (2002).
 - [14] B. Osberg, MSc. thesis (2009).
 - [15] M. H. Devoret, J. M. Martinis, D. Esteve, and J. Clarke, *Phys. Rev. Lett.* **53**, 1260 (1984).
 - [16] E. Jaynes and F. Cummings, *Proceedings of the IEEE* **51**, 89 (1963).
 - [17] R. R. Puri and G. S. Agarwal, *Phys. Rev. A* **33**, 3610 (1986).
 - [18] J. Ping, X.-Q. Li, and S. Gurvitz, *Phys. Rev. A* **83** (2011).
 - [19] J. Ping, Y. Ye, X.-Q. Li, Y. Yan, and S. Gurvitz, arXiv:1106.2901v2 (unpublished) (2011).
 - [20] J. M. Martinis, S. Nam, J. Aumentado, K. M. Lang, and C. Urbina, *Phys. Rev. B* **67** (2003).
 - [21] If we approximate the potential in Eq. (1) by a cubic potential, then the tunneling rate of the ground and the first excited states of the cubic potential can be computed by WKB approximation : $\Gamma_j = \omega_p/2\pi[432\Delta U/\hbar\omega_p]^{j+1/2}/\pi^{j/2} \exp[-36\Delta U/5\hbar\omega_p]$, where $j = 0, 1$ represent the ground $|g\rangle$ and first excited $|e\rangle$ states of the JJ, respectively. The ratio $\Gamma_e/\Gamma_g \approx 250\Delta U/\hbar\omega_p$. Here $\Delta U = 4I_0\phi_0/3\sqrt{2\pi}(1-I/I_0)^{3/2}$ is the barrier height and $\omega_p = 2^{1/4}\sqrt{2\pi I_0/C\phi_0}(1-I/I_0)^{1/4}$ is the plasma frequency of the cubic potential. The junction frequency ω_{eg} is related to the plasma frequency by $\omega_{eg} \simeq \omega_p(1-5\hbar\omega_p/36\Delta U)$ [20].